Article

In Silico Guided Nanoformulation Strategy for Circumvention of *Candida albicans* Biofilm for Effective Therapy of Candidal Vulvovaginitis

Nazia Hassan, Uzma Farooq, Ayan Kumar Das, Kalicharan Sharma, Mohd. Aamir Mirza, Suhail Fatima, Omana Singh, Mohammad Javed Ansari, Asgar Ali,* and Zeenat Iqbal*

Read Online

ACCESS | Metrics & More | Article Recommendations

ABSTRACT: Candidal vulvovaginitis involving multispecies of *Candida* and epithelium-bound biofilm poses a drug-resistant pharmacotherapeutic challenge. The present study aims for a disease-specific predominant causative organism resolution for the development of a tailored vaginal drug delivery system. The proposed work fabricates a luliconazole-loaded nanostructured lipid carrier-based transvaginal gel for combating *Candida albicans* biofilm and disease amelioration. The interaction and binding affinity of luliconazole against the proteins of *C. albicans* and biofilm were assessed using in silico tools. A systematic QbD analysis was followed to prepare the proposed nanogel using a modified melt emulsification−ultrasonication−gelling method. The DoE optimization was logically implemented to ascertain the effect of independent process variables (excipients concentration; sonication time) on dependent formulation responses (particle size; polydispersity index; entrapment efficiency). The optimized formulation was characterized for final product suitability. The surface morphology and dimensions were spherical and ≤300 nm, respectively. The flow behavior of an optimized nanogel (semisolid) was non-Newtonian similar to marketed preparation. The texture pattern of a nanogel was firm, consistent, and cohesive. The release kinetic model followed was Higuchi (nanogel) with a % cumulative drug release of 83.97 ± 0.69% in 48 h. The % cumulative drug permeated across a goat vaginal membrane was found to be 53.148 ± 0.62% in 8 h. The skin-safety profile was examined using a vaginal irritation model (in vivo) and histological assessments. The drug and proposed formulation(s) were checked against the pathogenic strains of *C. albicans* (vaginal clinical isolates) and in vitro established biofilms. The visualization of biofilms was done under a fluorescence microscope revealing mature, inhibited, and eradicated biofilm structures.
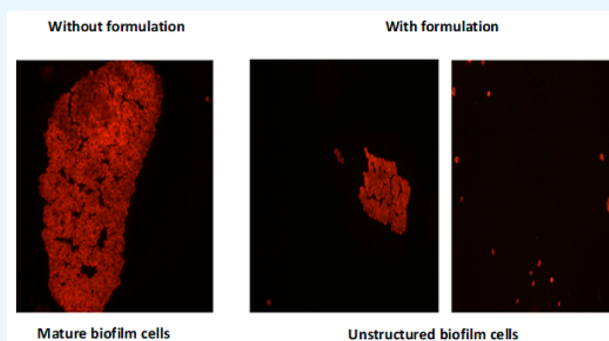
INTRODUCTION

Female reproductive health is a global concern, and candidal vulvovaginitis (CV) is reportedly a prevalent form of acute fungal infection that manifests as inflammation of both the vagina and vulva.[1] Associated with multispecies of *Candida* (*C. albicans*; *C. glabrata*; *C. tropicalis*; *C. krusei*) and lately with the emergence of epithelium-bound biofilm-forming disease spectra, it has earned the dubious distinction of being a pharmacotherapeutic challenge for both researchers and practitioners.[2]

A biofilm is a multistage, surface-attached, heterogeneous, diverse, microbial assemblage enclosed in an extracellular matrix (ECM). The ECM is self-produced by biofilm microbes and has a 3-dimensional (3D) establishment. The major components of ECM are extracellular polymeric substances and a microbial ecosystem (80%) which serves as a major virulent, resistant, tolerant, and persistent factor for CV manifestation.[3] The unicellular planktonic phase of a biofilm

allows for microbial dispersion and the colonization of new environments. This phase is most sensitive to antimicrobial agents. The multicellular sessile phase provides a more coordinated, stable space for biofilm proliferation and is highly resistant to antifungal therapy. The presence of persister cells—a dormant, phenotypic biofilm subpopulation (1%) fuel antimicrobial tolerance as well even at higher concentrations.[4]

The multifarious presentation of the disease and the associated limitations of the drug development pipeline to effectively readdress the same leaves enough space to ideate,
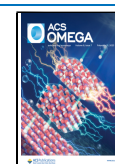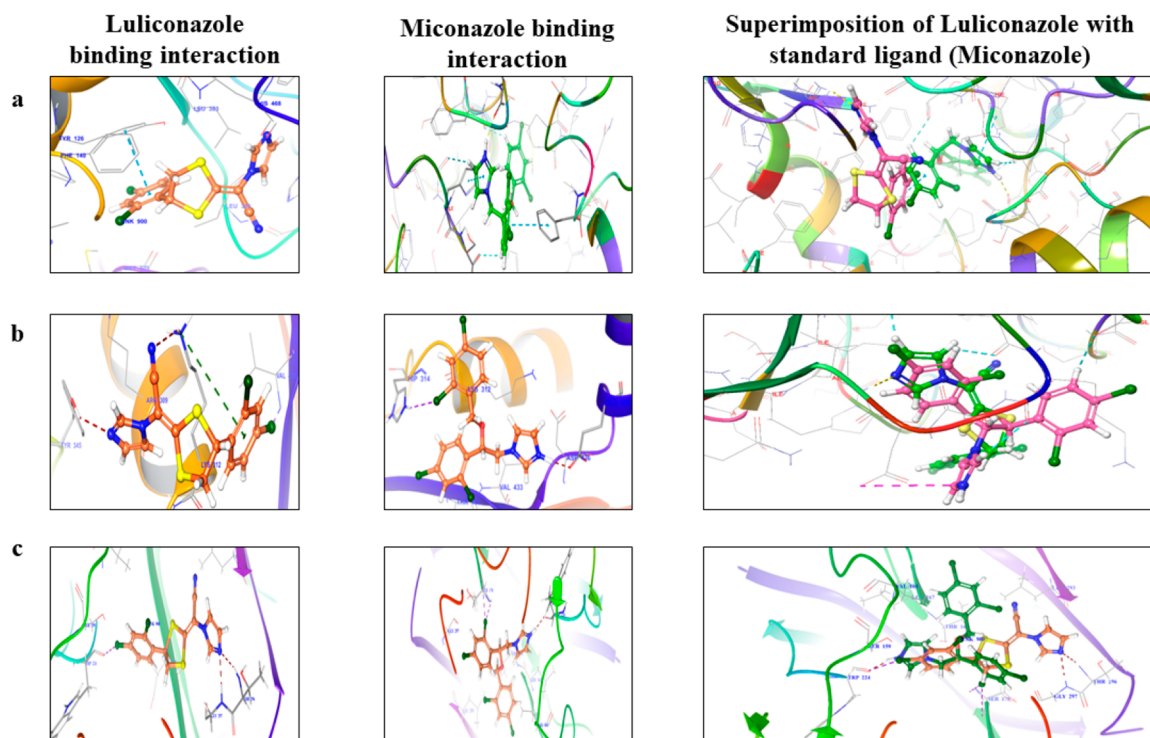
Figure 1. Molecular docking simulations of luliconazole and standard ligand against (a) lanosterol 14-α-demethylase receptor catalytic domain (PDB ID: 4ZDY); (b) Ppib protein receptor catalytic domain (PDB ID: 2RS4); (c) agglutinin-like Sequence3 receptors catalytic ligand-binding site (PDB ID: 4LE8).

design, and investigate well-researched formulation strategies targeted at biofilm disruption and subsequent antifungal action.[5] In pursuit of the above, the much-accepted research tools of in silico, molecular docking, and subsequent visualization of drug behavior in vivo were implemented to assess the suitability of luliconazole, a newer imidazole, for both its antifungal as well as biofilm arresting properties. Henceforth, the present work embarked on the in silico analysis of luliconazole against proteins of *C. albicans* and its biofilm. The performed molecular docking analysis may assist in predicting the crystallographic binding orientations and affinities of ligand (luliconazole) into a receptor-binding site of selected proteins, lanosterol-14-α demethylase, agglutinin like sequence-3 (ALS3), and peptidyl-prolyl isomerase-B (PPiB). The lanosterol-14-α-demethylase is a rate-limiting enzyme in cell wall biosynthesis, ALS3 are adhesin/invasin glycoproteins, and PPiB is a cyclophilin involved in the biofilm formation of *C. albicans*.[6,7] The computational validation of docking parameters was assessed against the established antifungal agents and standard drugs.

Niwano et al. first reported the inhibition potential of luliconazole against the sterol 14-α-demethylase of *C. albicans*, which later contributes to the drug mechanism of action.[8] Over time, luliconazole has offered a diverse antifungal activity against multispecies of *Candida*. The reported minimum inhibitory concentration (MIC) range of luliconazole against *C. albicans*, *C. glabrata*, *C. tropicalis*, and *C. krusei* was 0.031−0.13, 0.007−0.85, 007−2, and 0.008−1 μg/mL, respectively.[9] In comparison to other vaginal antifungal agents such as fluconazole, terbinafine, bifonazole, etc., the anticandidal activity (MIC) of luliconazole is 4−1000 times lower for the aforementioned multispecies.[10] The high lipophilicity of luliconazole further makes it suitable for NLC development

(high drug encapsulation) as well as vaginal delivery (interaction with lipid bilayer).[11]

Hence, the purported system is envisaged as a multiparticulate, mucoadherent, modified release (3M) transvaginal nanogel comprising of luliconazole-loaded nanostructured lipid carriers (NLCs) with attributes of high drug encapsulation, enhanced mucosal permeability, locoregional application, and better patient compliance.[12]

The antifungal susceptibility of luliconazole and the purported formulation (nanogel) were evaluated against the clinical isolates of *C. albicans* (MIC) and their established biofilms (biofilm assay). The biofilm assay cumulates two different parameters, i.e., minimum biofilm inhibitory concentration (MBIC) and minimum biofilm eradication concentration (MBEC).[13] Such a well-researched drug delivery system could be a biopharmaceutical game-changer and lead to successful elimination of *C. albicans* along with its biofilm cells (planktonic, sessile, persister) and offers dependable relief to CV patients.

Another important aspect of this proposal is its socioscientific approach, which additionally focuses on providing brief knowledge about a much-neglected area of female reproductive health.

■ RESULTS AND DISCUSSION

Molecular docking is supposedly advanced in silico tool for the customization of drug delivery systems to ensure adequate translation into clinical settings. Recently, an appreciable percolation into the formulation research domain has been employed in concurrence with the understanding of the disease, the exploration of the target site, and the adaptation of a strategic formulation design. Such an informed approach to drug formulation design is eventually an assurance of its
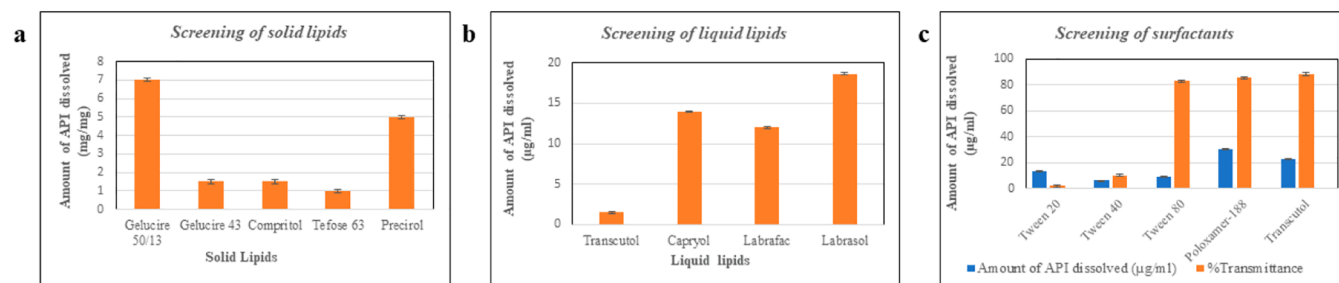
Figure 2. Preliminary excipient screening: (a) solid lipids; (b) liquid lipids; (c) surfactants.

Table 1. QTPP and CQAs for a Nanogel

QTPP	Target	Justifications
Formulation	Nanostructured Lipid Carriers, NLCs	Incorporation of a hydrophilic drug, sustained and locoregional release, mucosal adhesion, increased drug stability, and payload
Route of administration	Transvaginal	Minimal systemic side effects and interactions, avoidance of first-pass metabolism and enzymatic degradation, self-medication, rapid drug absorption, and quick onset of action
Anticandidal potential	Should be better than the already available form	The limited success of available treatment tools to target both fungal and biofilm components of *C. albicans* in and as a single formulation
Stability	No visual signs of non-uniformity/cracking/breaking	The efficiency of the formulation depends on lipid-surfactant phase/blend, and particle size, and hence, they are imperative to develop a stable formulation

CQAs	Target	Justifications
Mean particle size	Should be ≤300 nm	The nanoparticle size may offer enhanced mucus permeation, retention, and adhesion which in turn support the transvaginal delivery and application. Also, nanosized particles may have an increased surface area which subsequently increases drug solubility and bioavailability
Poly dispersity index (PDI)	Less than 0.5	PDI refers to the size distribution of particles which may affect formulation uniformity (homogeneous and heterogeneous) and drug distribution. A high PDI (>0.5) signifies particle agglomeration, and a low PDI (<0.2) refers to particle disintegration. The disintegrated particles could lead to drug expulsion and formulation instability
Entrapment efficiency (EE)	Higher	The amount of drug entrapped in a lipid matrix refers to entrapment efficiency. It is a quantitative measurement often calculated in percentage (%). A high %EE higher will be the drug loading and low application dose

success in in vitro and in vivo conditions and would create a fine balance of IVIVC correlation. For the present molecular docking screening, luliconazole showed the highest docking score and superimposition with standard ligand against lanosterol-14-α demethylase, ALS3, and PPiB (Figure 1a–c).

Luliconazole is a potent anticandida drug with an appreciable MIC range of 0.031–0.13 μg/mL against *C. albicans* (the predominant causative agent of CV).[10] It has not been explored commercially for vaginal application but does have significant literature support for the same. Moreover, the increasing resistance against conventional therapeutics (azole antifungals) such as fluconazole, miconazole, etc. necessitates the focus to shift to a newer class of antifungal agents, imidazoles.[14] Further, the high lipophilicity compliments the fabrication of lipid-based nanoformulations for intravaginal application. Lastly, a skin-friendly, nontoxic profile makes it an obvious choice.[15]

UV. The UV analysis of API with methanol alone and methanol: VFS (5:5) yielded concordant observations. The results were obtained in triplicate as mean value (μg/mL) ± SD.[16] The API/drug solution in both methanol and methanol: VFS was found to be stable for 1 week when assessed in terms of environmental factors (light, temperature, humidity, air) and drug-related factors.

Excipient Screening. Gelucire 50/13 and labrasol have yielded high drug solubilization (Figure 2a,b) and were selected as solid and liquid lipids, respectively. Gelucire 50/13 is a vehicle from the gelucire family and consists of mono/di/triglycerides, polyethylene glycol (PEG)-32, and mono/diesters of palmitic and stearic acids. It is in the form of oval pellets with a melting range of 46–51 °C and HLB 11.

Labrasol consists of mono/di/triglycerides, PEG-8 (MW 400), and mono/diesters of caprylic and capric acids. The product form is liquid, with viscosity (20 °C) of 80–110 mPa.s and HLB 12.[17] Both the selected lipids are well cited to improve solubilization and bioavailability of poorly soluble drugs, especially in oral formulations. The main functionalities focusing on the present work include formulation (transvaginal gel) stabilization, thickening, enhanced permeation, and drug release modulation.[18]

The surfactants were selected based on two attributes vis-à-vis drug-solubilization capacity and % transmittance. The obtained results indicated a high drug solubilization and % transmittance value for Tween 80 and Transcutol HP (Figure 2c). Tween 80 (polyethylene glycol sorbitan monooleate) is a nonionic, viscous, and water-soluble surfactant/emulsifier (HLB-15). Transcutol P (diethylene glycol monoethyl ether) is a highly purified solvent, solubilizer (HLB-4 ± 0.2), and permeation enhancer in topical formulations.[17] The high % transmittance for both surfactants signifies high dispersion and low globule size, both of which are crucial attributes for fabricating a nanometric formulation. Also, the nonionic nature of Tween 80 may impart an electrostatic repulsion and stearic stabilization to the designed formulation, which reduces particles agglomeration as well.[11,19]

Binary Lipid Phase. The binary lipid ratio of 7:3 was found to be compatible in terms of homogeneity, turbidity, and clarity[19] and was further selected for formulation development.

QbD Analysis. *Defining Quality Target Product Profile (QTPP) and Identifying Critical Quality Attributes (CQAs).* QTPP is an important element for the design and development of the formulation/product. For purported formulation, QTPP
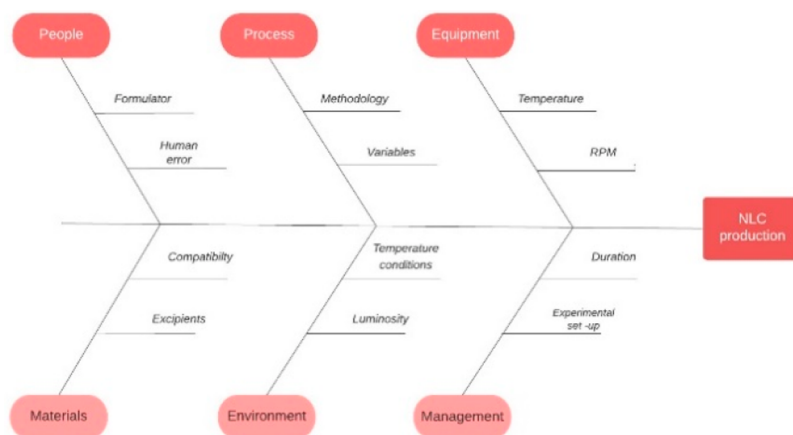
Figure 3. Potential high-risk formulation and process attributes, their causes, and effects.

Table 2. BBD Formulation Designs for a Nanogel Optimization

Std	Run	Factor 1 A: Total lipid concentration (%w/v)	Factor 2 B: Total surfactant concentration (%w/v)	Factor 3 C: Sonication time (sec)	Response 1 Particle size (nm)	Response 1 PDI	Response 3 EE (%)
16	1	3	3	60	197.5	0.22	79.6
11	2	3	1	90	262.5	0.116	72.46
8	3	5	3	90	319.5	0.193	74.4
10	**4**	**3**	**5**	**30**	**207.3**	**0.206**	**83.7**
7	5	1	3	90	212.4	0.128	69.8
1	6	1	1	60	142.4	0.185	65.9
15	7	3	3	60	197.5	0.22	79.6
3	8	1	5	60	151.6	0.133	68.1
9	9	3	1	30	252.6	0.234	86.43
17	10	3	3	60	197.5	0.22	79.6
4	11	5	5	60	234.2	0.198	79.7
6	12	5	3	30	287.9	0.204	88.3
5	13	1	3	30	142.4	0.185	64.2
14	14	3	3	60	197.5	0.22	79.6
13	15	3	3	60	197.5	0.22	79.6
2	16	5	1	60	268.8	0.241	86.47
12	17	3	5	90	230.4	0.217	73.36

serves as both design criteria and a starting point for identifying the CQAs, critical material attributes (CMAs), and critical process parameters (CPPs). CQAs are formulation-based physical, chemical, biological, and microbiological characteristics that ideally should be within a predetermined limit or range to ensure the desired quality of a final product. For the present formulation, both QTPP and CQAs were compiled in Table 1 with related targets and justifications.[20]

Initial Risk Assessment and Identification of Critical Material Attributes (CMAs) and Critical Process Parameters (CPPs). The presented Ishikawa diagram (Figure 3) enlists, identifies, and optimizes potential high-risk attributes, CMA and CPPs, and studies their effect on CQAs to ensure the desired quality of the purported formulation.[21]

Response Surface Methodology: Formulation Development and Optimization. The nanogel was formulated by modified melt emulsification−ultrasonication−gelling method. The optimization was carried out by employing a response surface methodology (BBD). It is a system-generated tool to determine, represent, and assess the cause-and-effect relationship between dependent formulation responses—particle size, PDI, EE, and independent process variables such as total lipid, surfactant concentration, and sonication time. The influence of variables on responses was represented as a 3D quadratic

graph. For the purported analysis, 17 runs (formulation designs) were designated (Table 2), and formulation F4 was selected as the optimized formulation with particle size 207.3 nm, PDI 0.206, and % EE 83.7% (Figure 4). A brief discussion of each variable and response is presented below:

Particle size and distribution are key characteristics of NLCs as they majorly influence stability, solubility, drug release rate, biodistribution, and cellular uptake. The usual diameter range for an NLC is 10−1000 nm. However, for site-specific delivery, a much finer <600 nm is preferred. The purported formulation is specifically designed for a locoregional application to target the active components at the site of infection (CV) with no or negligible systemic absorption to prevent any undesirable or unwanted side effects. A much smaller particle size of <300 nm often exhibits the desired diffusion and transport kinetics through a transvaginal route.[22] The size of NLCs may also govern microbial interaction and antimicrobial activity. This attribute is of crucial importance as the delivery system is proposed to preclude a biofilm-associated fungal infection, CV. The prepared BBD formulations offer a particle range envisaged to interact and bind to the *C. albicans*-surface/biofilm following permeation into the fungal-membrane/biofilm to elicit a desired anticandidal and antibiofilm potency.[12]
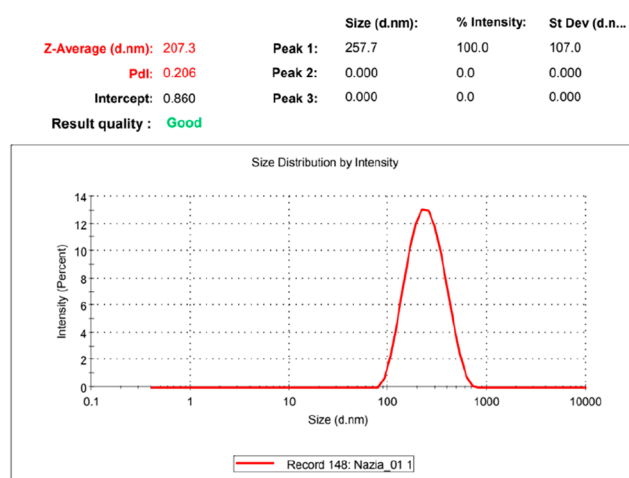
Z-Average (d.nm): 207.3
PdI: 0.206
Intercept: 0.860
Result quality : Good

	Size (d.nm):	% Intensity:	St Dev (d.n...
Peak 1:	257.7	100.0	107.0
Peak 2:	0.000	0.0	0.000
Peak 3:	0.000	0.0	0.000

Size Distribution by Intensity

Record 148: Nazia_01 1

Figure 4. Zeta sizer graph representing the particle size and PDI of an optimized formulation.

The influence of independent variables on dependent responses was represented as a 3D quadratic graph (Figure 5). The selected independent variables greatly affect the particle size of the formulation. As highlighted in 3D graphs particle size increases with an increase in lipid concentration due to longer chain lengths among the molecules. However, with the increase in surfactant concentration the particle size decreases as the nonionic nature of surfactants may impart electrostatic repulsion and stearic stabilization among the particles which contribute to low aggregates and smaller droplet size. The less sonication time also prevents lipid particles from coalescing into large droplets.[11]

PDI mainly represents particle homogeneity within a given sample, and its numerical value ranges from 0.0 (highly monodisperse) to 1.0 (highly polydisperse). A high PDI could be due to sample agglomeration/aggregation during isolation or analysis. For lipid-based nanoformulations, a PDI of ≤0.3 indicates a monodisperse particle size population.[23,24] All of the prepared formulations fall into a similar range (Table 2). As highlighted in 3D graphs, PDI decreases with a decrease in sonication time as the latter contributes to low agglomeration among particles. The concentration of surfactants has a negligible effect on PDI.[29]

The lipid−drug solubility parameter influences the drug entrapment efficiency; i.e., a high amount of lipid entrapped more drug to yield a high % EE. Thereby, a high amount of
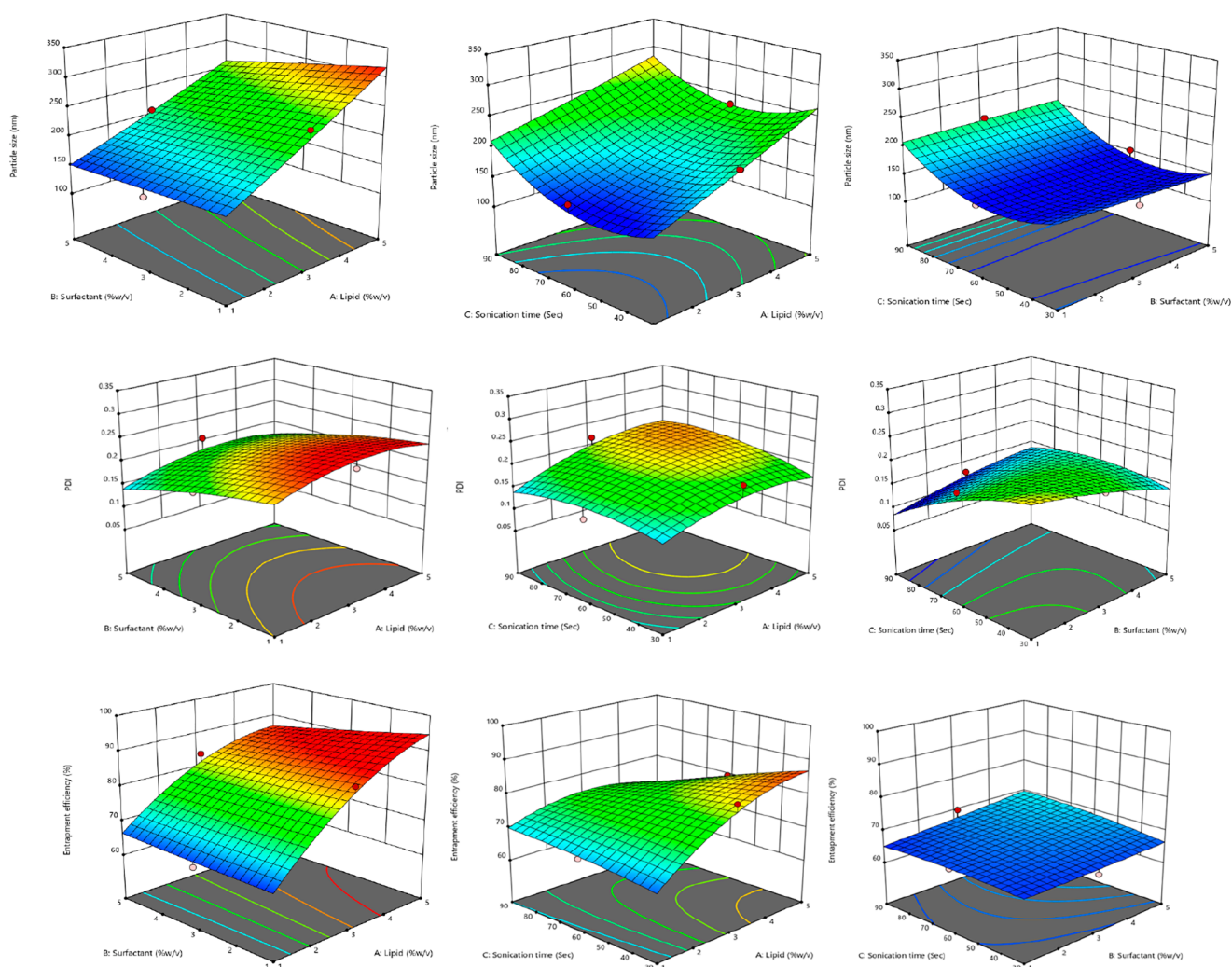

Figure 5. 3D-BBD graphs representing the effect of independent process variables on dependent formulation responses.

entrapped API may subsequently influence the anticandidal potential of a designated formulation. The concentration of surfactant and sonication time has a low or only slight effect on % EE.[23]

The polynomial equations obtained for each dependent formulation response in terms of coded factors are as follows:

$$\text{Particle size} = +197.50 + 57.70A - 12.85B + 16.83C$$
$$- 10.95AB - 9.60AC + 3.30BC + 2.0A^2$$
$$- 0.3000B^2 + 41.00C^2$$

$$\text{PDI} = +0.2200 + 0.0256A - 0.0027B - 0.0219C$$
$$+ 0.0023AB + 0.0115AC + 0.0323BC - 0.0233A^2$$
$$- 0.0075B^2 - 0.0193C^2$$

$$\text{Entrapment efficiency} = +79.60 + 7.61A - 0.8000B$$
$$- 4.08C - 2.24AB - 4.87AC$$
$$+ 0.9075BC - 4.69A^2 + 0.1275B^2$$
$$- 0.7400C^2$$

Characterization of an Optimized Formulation.

Electron Microscopy. The micrograph of SEM (Figure 6a)
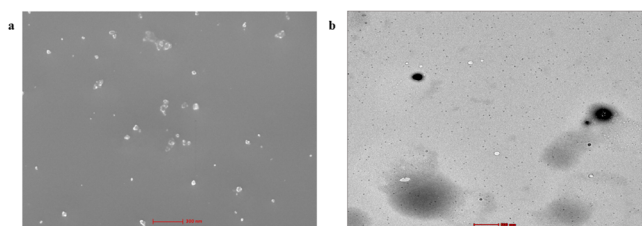

Figure 6. (a) SEM; (b) TEM micrographs of an optimized formulation.

provides a detailed image of an optimized NLCs dimension (<300 nm) and morphology (slightly spherical). As highlighted in TEM micrographs (Figure 6b), a less dense external nonlipid core corresponds to the aqueous-surfactant layer surrounded by a denser lipid–drug core. The presence of the aqueous-surfactant layer is imperative to stabilize the lipid core region, thus negating unnecessary drug expulsion and mobilization.[12]

Rheology Assessment and Texture analysis. The optimized nanogel was found to be a complex viscoelastic material

that shows properties of both solids and liquids in response to force, deformation, and time. The flow curve of nanogel (Figure 7a) shows a sheer-thinning flow behavior which reflects that the gradient of the shear stress decreases, and sample viscosity becomes lower at higher shear rates. For non-Newtonian fluids (present formulation) the viscosity is a function of shear rate and is often termed as apparent viscosity (ηA). A high viscosity may contribute to sample adhesion, and a low viscosity may influence sample spreadability at the application site.[25] For an optimized nanogel the apparent viscosity is inversely proportional to the shear rate; i.e., viscosity decreases greatly with increasing shear rate. This response reveals thixotropy, and it implies that the structure in the material (gel sample) breaks down over time and needs time to recover. Hence, it can be presumed that with applied shearing the viscosity will be low, aiding material spreadability, and with the cessation of rubbing/shearing the viscosity will be high to increase contact/residence time of formulation at the application site.[26] For purported formulation a disposable applicator can be devised to dispense the medication into the vagina (cervix) where it is then absorbed, thus negating shearing, rubbing, etc. to aid higher viscosity. Comparatively, a marketed gel preparation (Figure 7b) with an external, disposable applicator was also evaluated on similar parameters and has revealed concordant observations.

Texture Profile. To measure the extrudability a texture profile has been observed on typical parameters of firmness, consistency, cohesiveness, and work of cohesion. Extrudability can be defined as a force required to push/expel/dispense/extrude the formulation from an outlet (external packaging, applicator).[27] Owing to the physical nature of an optimized nanogel a compression–extrusion (back-rig) test was applied to quantify its extrudability (Figure 8). The firmness of a prepared gel signifies its structural integrity upon application of an external compressive force. A firm product can be described as one that is moderately resistant to deformation/compression. Generally, the higher the compression force the firmer the sample and the more its structural integrity. At a trigger force of 5.0g, the firmness of the optimized gel was found to be 361.93g. The variable of consistency concerning applied force (g) and time (s) was found to be 671.66 g·s. The obtained consistency value relates to the thickness/viscosity of a gel (semisolid) preparation which affects product expulsion/flow from the external packaging and also its spreadability and residence time at the application site. The negative area of the graph represents the total resistance to an applied trigger force
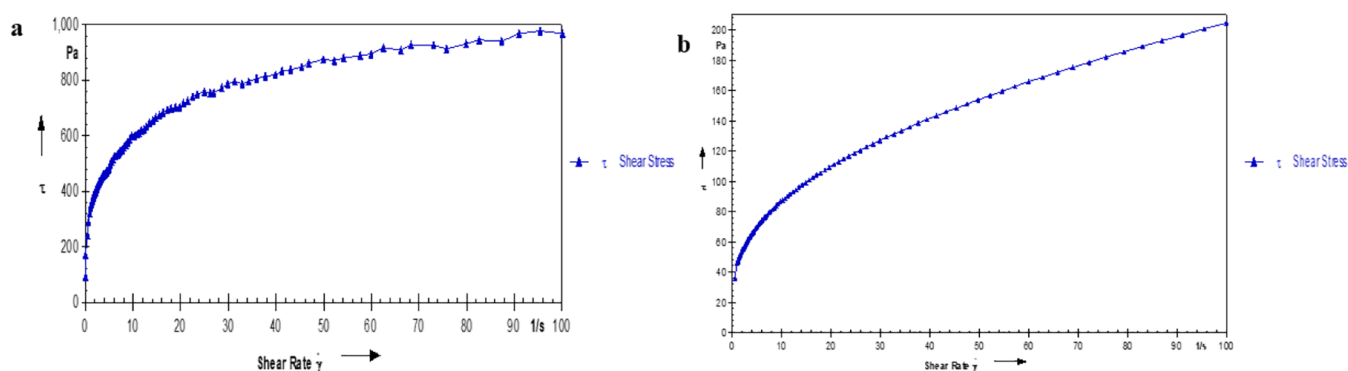

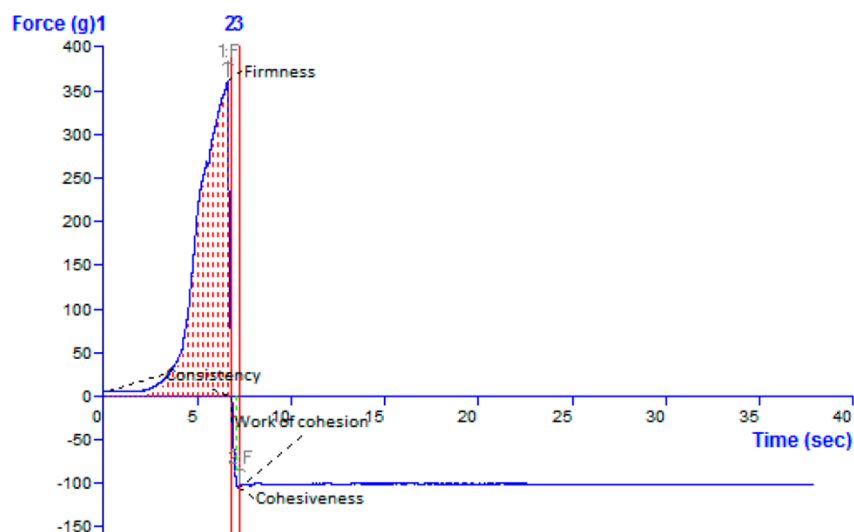**Figure 7.** Rheology profile: (a) optimized nanogel; (b) marketed gel.

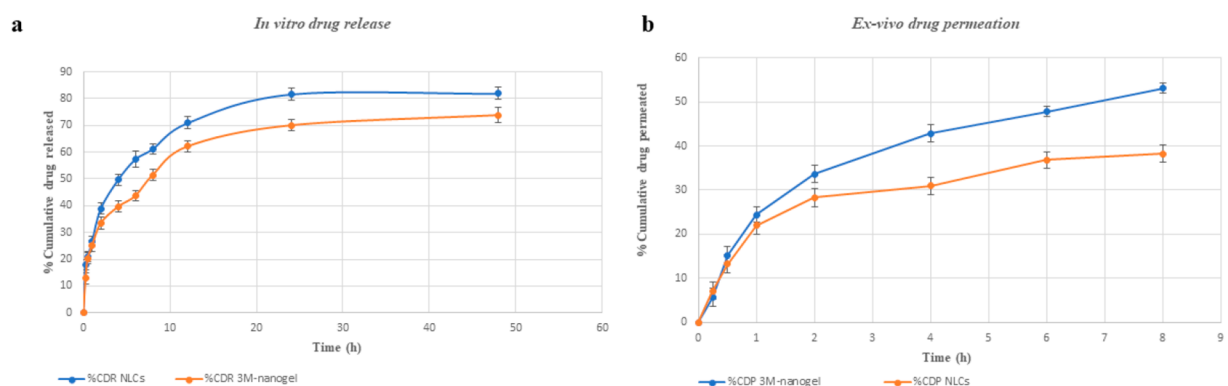**Figure 8.** Texture profile of an optimized nanogel.

Figure 9. (a) % Cumulative drug release; (b) % cumulative drug permeation profile of optimized NLCs (non-gel preparation) and nanogel.

and is referred to as cohesiveness, which was found to be −105.34g for an optimized nanogel. It can also be referred to as a sample intermolecular attraction by which the material coheres or stick together. For purported formulation, a high cohesion (more negative) is an imperative characteristic since a pressure-sensitive adhesion is required to strongly hold the gel together by itself and with the vaginal-mucosal lining without tearing. The cohesion coefficient that implies how well the product withstands deformation concerning time is a work of cohesion, and it was observed to be −29.73g.s. The textural properties are a basic prerequisite to ensure formulation stability under tensile stress, consistency throughout its shelf life, ease of applicability, and patient compliance.[11,28]

The visual appearance of an optimized nanogel was homogeneous, and the pH and % drug content values were 4.5 ± 0.5 (concordant to normal vaginal pH balance) and 0.86 ± 0.02% (w/w) respectively.

In Vitro Drug Release. The cumulative drug release of an optimized nanogel and NLCs was found to be 83.97 ± 0.69% and 61.82 ± 0.70% in 48 h (Figure 9a). Since the prepared formulation comprises a semisolid vehicle with suspended drug particles that may ensure maximum thermodynamic activity, the release kinetic model followed was Higuchi. The prepared nanogel was envisaged to maintain a therapeutic concentration of the drug in a vaginal milieu. The nanometric particle range (NLCs) may provide a higher surface area for solubilization

which subsequently enhances the dissolution rate and solubility of a drug. The translation of NLCs as NLC gel (nanogel) adds various advantages vis-à-vis enhanced vaginal-mucosal adhesion as the neat NLCs in a suspension are amenable to easily washing off. Since the anatomical structure of the application site requires high mucoadhesion to aid formulation retention and support prolonged drug release the nanogel seems an improved option.[29]

In many scenarios, a depletion of drugs from the vehicle is more frequent than the release or passing of drugs across the desired therapeutic area due to a lower thermodynamic driving force. Thus, for the present formulation, an average applied thickness of an order of 20 μm was suggested so that even depletion of a small quantity of the drug might produce a sharp concentration gradient in the proposed vehicle (nanogel) which may increase diffusivity across a membrane (lipid bilayer) and ensure a better pharmacological performance.[27,30]

Ex Vivo Drug Permeation. The % cumulative drug permeated through an optimized nanogel and NLCs was found to be 53.148 ± 0.62 and 38.42 ± 0.60% in 8 h (Figure 9b) across a goat vaginal membrane. Similar to the observation of the *in vitro* drug release study the nanogel has shown a high permeation due to its increased viscosity which further supports mucoadhesion, retention, and contact time with the membrane. The presence of triethanolamine (only nanogel) and Transcutol as skin permeation enhancers further

corroborate the above results. The ability of permeants to saturate the intercellular lipid domain allows a greater amount of drug to partition into the skin layers.[28]

Vaginal Irritation Study. There were no mortalities in any of the groups during the application period. The visual examination of each rat was done to assess the severity of erythema and edema (Table 3). Erythema is a superficial skin

Table 3. Vaginal Irritation Profile of an Optimized Nanogel[a,b]

Group (n = 2)	Erythema	Edema
Control (no formulation)	0	0
Nanogel (formulation)	1	1
Placebo gel	1	1

[a]Erythema scale: 0 = none, 1 = very slight (barely perceptible), 2 = well-defined (perceptible), 3 = moderate (highly perceptible), 4 = severe (beet redness). [b]Edema scale: 0 = none, 1 = very slight (barely perceptible), 2 = well-defined (swollen area with edges), 3 = moderate (swollen area raised ~1 mm), 4 = severe (swollen area >1 mm and extending).

rash/redness which usually occurs in response to drugs, diseases, or infection. The major cause of erythema is injured or inflamed blood capillaries. The severity of erythema ranges from mild to life-threatening. Edema refers to a condition of build-up fluids in the body which causes the affected tissue or area to become swollen.[31] Although the visual examination of each rat revealed no significant signs of vaginal or vulva irritation, discharge, or bleeding, the formulation and the placebo-treated group have shown very slight erythema and edema (barely perceptible). This could be attributable to a mild application site reaction as compared to the no-formulation (control) group.

Histological Assessment. The histological assessment did not reveal any corresponding findings from the vaginal irritation study. The vaginal and cervical tissues of the formulation-treated group were similar to those of the control-treated groups. The microscopic examination revealed an intact vaginal and cervical epithelium (Figure 10a) in all the
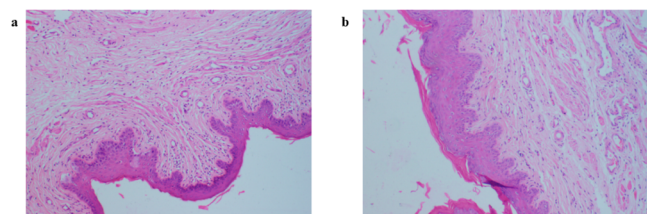

Figure 10. Histological assessment of (a) control; (b) formulation treated groups.

groups. In the formulation-treated group, however, a slight application-site disruption of vaginal/cervical tissues was observed due to the bursting of surface capillaries (Figure 10b). The disruption is local and not much profound keeping in view very slight erythema and edema (barely perceptible) as observed in vaginal irritation studies.[32]

Anticandidal Activity. The obtained MIC of luliconazole was 0.031 μg/mL which falls under the reported MIC range against *C. albicans*: 0.031−0.13 μg/mL.[10] The MIC of an optimized formulation (NLC) was found to be 0.124 μg/mL. Notably, no formation of cell clusters or buttons was observed

in any of the tested drug and formulation concentrations. This could be deduced that even the lowest drug concentration can produce a visible inhibition of yeast growth owing to its broad spectrum of anticandidal activity. The encapsulation in a nanolipid carrier has not affected drug anticandidal potential as the observations were concordant. In both the control and sterile control group fungal growth was observed, i.e., no inhibition. The interaction of luliconazole with lanosterol-14α demethylase facilitates ergosterol depletion to increase cell membrane permeability for the accumulation of toxic intermediate sterols which inhibits fungal growth and causes subsequent cell death.[6]

Antibiofilm Activity. The antibiofilm activity of luliconazole was evaluated in terms of MBIC and MBEC. The lowest API concentration at which the developed biofilm was inhibited is MBIC, and it was found to be 0.488 μg/mL. The MBEC of 0.976 μg/m was taken as the lowest API concentration responsible for 90% or complete eradication of a biofilm compared to growth controls.[33] The optimized formulation has shown antibiofilm activity similar to plain drug solution in DMSO (inert solvent). In both the control and sterile control group fungal growth was observed, i.e., no biofilm inhibition/eradication. The interaction of luliconazole with ALS3 and PPiB at the molecular level played a major role in biofilm inhibition and eradication. Since ALS3 are fungal adhesin/invasin glycoproteins and PPiB is a cyclophilin involved in biofilm formation the API interaction with both of them may combat the cells of biofilm. This may lead to unstructured biofilms as highlighted in fluorescence microscopy images.[34,35]

Fluorescence Microscopy. To corroborate the findings of antibiofilm activity through the microtiter plate method, fluorescence microscopy was performed using the drug concentrations determined by the MBIC and MBEC assay. Three different sets of glass slides were prepared, and the microscopic examination of each set revealed distinct findings. The mature biofilm formed on the first set of slides has a dense, multicellular structure (Figure 11a). On the second set of slides, no substantial biofilm formation was observed, indicating that the formulation successfully prevented biofilm maturation (Figure 11b). Biofilm eradication was observed on the third set of slides as smaller fragments of lesser density and the absence of any large dense structure, indicating disruption of earlier formed biofilm (Figure 11c).

The biofilm inhibition and eradication properties depend on the capacity of the formulation to prevent adhesion, penetration, and perturbation of the mature biofilm layer and to kill a considerable percentage of slow or nongrowing (SONG) cells in the biofilm.[36] As discussed earlier, the interaction of luliconazole with ALS3 and PPiB at the molecular level has played a major role in biofilm inhibition and eradication. However, the exact mechanism of biofilm inhibition and eradication of the present formulation(s) needs further elucidation through additional studies.

■ CONCLUSION

Candidal vulvovaginitis has been found to be a difficult-to-treat female reproductive tract infection resulting in poor Quality of Life (QoL). The predominant causative agent is *C. albicans* responsible for 80−95% of the total global cases and biofilm-associated disease spectra as well. The limited success of available treatment tools to target both fungal and biofilm components of *C. albicans* further complicates the patient's situation. Thus, the fabrication of a tailored nano-based drug
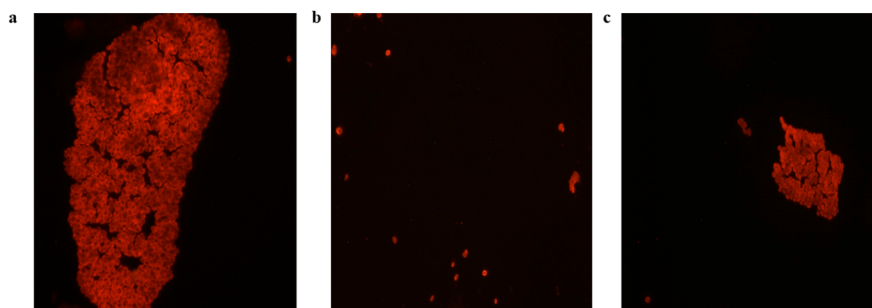
Figure 11. Fluorescence microscopy visualization of biofilm structures: (a) mature; (b) inhibited; (c) eradicated.

delivery to target the site of action (vulva and vagina), inhibit/eradicate *C. albicans* biofilm, and mitigate infection makes research as well as commercial sense. The purported research reports the antibiofilm activity of luliconazole for the first time against clinical isolates of *C. albicans* in terms of MBIC and MBEC. The prepared nanogel is pharmaceutically active and easy to prepare, and the bipronged activity of luliconazole could be a groundbreaking research endeavor. Also, the said research work would expectably bring awareness into the public domain regarding female reproductive health, its compromised status, and how good research and a therapeutic approach would amicably redress the challenges associated with CV and yield an effective long-term therapy tool.

■ MATERIAL AND METHODS

The ex gratia samples of drug and lipids were provided by Sun Pharmaceuticals, Gurgaon, India, and Gattefosse, France, respectively. The surfactant samples carbopol (grade 974) and triethanolamine were procured from Sigma-Aldrich, India. All other chemicals and reagents used were of analytical grade and were used without further purification.

Preformulation Studies. *In Silico.* Molecular docking of the selected drug was performed at the lanosterol-14-α-demethylase (PDB ID: 4ZDY), agglutinin-like sequence-3 (PDB ID: 4LE8), and peptidyl-prolyl Isomerase-B (PDB ID: 2RS4) receptor catalytic ligand-binding site, Maestro, version 9.6, Schrodinger software suite. For the validation of docking parameters, the standard ligand, Miconazole (Over-the-Counter Intravaginal Agent) was selected.[37] The docking simulations will help to better understand the drug−protein (ligand) interaction at the molecular level. The ligands were sketched in a 3D format using a building panel and were prepared for docking using the ligprep application. The apoprotein was taken from the Protein data bank (PDB ID: 2RS4) and applied in the protein preparation wizard to remove the solvent and add hydrogen and energy minimization. Site map analysis was done to obtain the active site of a protein and a grid was prepared around active amino acid residues. All compounds were docked using Glide extra-precision (XP) mode keeping with up to three poses saved per molecule.

UV Spectral Analysis. A previously described method to assess drug solubility and stability in methanol and vaginal fluid simulants (VFS) was followed. The composition of VFS was kept similar to that proposed by Tietz et al., with few modifications.[38] For stock preparation, 5 mg of the drug was dissolved in equal parts of methanol and VFS. The prepared serial dilutions, API (5−25 μg/mL) were analyzed at λ_{max}, 296.5 nm, UV−visible spectrophotometer, UV-1601, Shimadzu. The results were obtained in triplicate as mean value (mg/

mL) $\pm$ SD. Following analysis, the drug solution stability concerning environmental factors was also assessed.[16]

Excipient Screening. Solid Lipids. In a molten lipid phase (10 °C above the melting point) an incremental quantity of drug (1 mg) was added until the point of saturation using a magnetic stirrer, 100 rpm, Remi Instrument Ltd., Mumbai, India. The lipids solubilizing maximum drug quantity were selected for further studies. The results were obtained in triplicate as mean value (mg/mg) $\pm$ SD.[11]

Liquid Lipids. 2 mg of drug samples was added to 2 mL of selected lipids and kept on unremitted stirring (200 rpm) for 24 h using a mechanical shaker at 25 °C to attain equilibrium. The samples were then centrifuged for 30 min to obtain a supernatant. To evaluate the amount of dissolved drug the supernatant samples were separated, solubilized in methanol, and analyzed at λ_{max}, 296 nm, UV−visible spectrophotometer (UV-1601, Shimadzu).[19] The results were obtained in triplicate as mean value (μg/mL) $\pm$ SD.

Surfactants. 2 mg of drug samples was added to 2 mL of selected surfactants and kept on unremitted stirring (200 rpm) for 24 h using a mechanical shaker at 25 °C to attain equilibrium. The samples were then centrifuged for 30 min to obtain a supernatant. To evaluate the amount of dissolved drug the supernatant was dissolved in methanol and analyzed at λ_{max}, 296 nm, UV−visible spectrophotometer (UV-1601, Shimadzu). The surfactant samples were also tested for % transmittance.[11,19] The results were obtained in triplicate as mean value (μg/mL) $\pm$ SD.

Binary Lipid Phase. A ratio of solid to liquid lipids was visually evaluated as 1:9, 8:2, 7:3, 6:4, and 5:5 on parameters of homogeneity, turbidity, clarity, and phase separation.[11,19]

Formulation Development. *QbD Analysis.* A systematic approach to better understand formulation variables and their effect on the corresponding factors.[20] For purported work the QbD was established as follows:

- Defining QTPP and identifying the CQAs

- Initial risk assessment, identification of CMAs and CPPs

The development of a purported nanogel involves multistage production and variables such as lipid (solid as well as liquid), surfactant concentrations, speed, temperature, and RPM. Assessing one variable at a time is a difficult premise and time-consuming and would often not reveal precise formulation outcomes; thus, a systematic QbD analysis is a must to achieve the desired formulation product.[39] An initial risk assessment was carried out using an Ishikawa (fishbone) diagram to assess the cause-and-effect interrelationships between high-risk formulation/process variables and their attributes (CQAs).[21]

Selection of Suitable Methodology. The proposed transvaginal nanogel was formulated using a modified melt emulsification−ultrasonication−gelling method.[22] The selected lipids were separately melted at 10 °C above their melting points and mixed to prepare a clear binary lipid phase, BLP (7:3). An accurately weighed amount of API was dissolved in the above mixture, thus constituting a *lipid drug phase.* For preparing an *aqueous surfactant phase*, both the surfactant and cosurfactant were accurately weighed and mixed with double distilled water maintained at BLP temperature. The prepared *aqueous surfactant phase* was added to the *lipid drug phase* dropwise over a magnetic stirrer (Remi Instrument Ltd., Mumbai, India). The pre-emulsion thus formed was subjected to sonication (probe sonicator) and further cooled at room temperature to form NLCs. A gelling agent (Carbopol 974P NF) and triethanolamine were added to the prepared NLCs with varying concentrations (0.5, 1, 1.5%) to form the purported nanogels.[30]

Formulation Optimization. *Embarking Design Space Using Response Surface Methodology (RSM).* BBD (Design-Expert 12.0.3, Stat-Ease, Inc.) is a statistical design space created using response surface methodology to predict and analyze the effect of selected independent process variables over the dependent formulation responses.[40] For the present formulation the selected independent process variables were total lipids concentration (% w/v), total surfactants concentration (% w/v), and sonication time (s). The dependent formulation responses selected were particle size (nm), polydispersity index (PDI), and entrapment efficiency (%).[41,42]

Characterization of an Optimized Formulation. *Particle Size and PDI.* The suitably diluted suspensions (lyophilized NLCs) were analyzed using Dynamic Light Scattering, Zetasizer (Nano ZS90, Malvern Instruments Ltd., Worcestershire, UK), implemented with DTS software to measure the particle size and PDI.[43,44]

Entrapment Efficiency (EE). The NLCs samples were centrifuged at 10000 rpm for 45 min, High-Speed Centrifuge (Sigma-3K30, Sigma Laboratory Centrifuges, Germany). To measure the amount of drug the supernatant samples were diluted and analyzed at λ_{max}, 296 nm, UV−visible spectrophotometer (UV-1601, Shimadzu), and the % EE was calculated using the following equation[43,45]

$$\%EE = Dt - Ds/Dt \times 100$$

where Dt is the total amount of drug present in NLCs samples and Ds is the amount of drug entrapped in the supernatant.

Electron Microscopy. *Scanning Electron Microscope (SEM).* A gold-coated sample of a suitably diluted suspension (optimized formulation) was examined to evaluate particle surface morphology using SEM imaging, Zeiss EVO40, Carl Zeiss NTS (North America).[29]

Transmission Electron Microscope (TEM). A carbon-coated, negative stained grid of diluted suspension (optimized formulation) was examined for particles surface morphology and dimensions using CRYO-TEM imaging (Thermo-Scientific).[29]

Rheology and Texture Profile. The rheology of an optimized nanogel was evaluated on attributes of spreadability, homogeneity, and mean extrudability using a rheometer (Physica MCR 101, Anton Paar). The formulation was visually evaluated on physical parameters as well such as breaking, homogeneity/presence of aggregates, changes in color, odor, etc. The viscosity and pH were also determined using a

Brookfield viscometer and pH meter. The drug content analysis of a nanogel was also done at λ_{max}, 296 nm, UV−visible spectrophotometer (UV-1601, Shimadzu).[25]

The tensile strength of an optimized nanogel was determined by using a texture analyzer (5 kg-loaded cells, TA.XT2, Stable Micro Systems, Godalming, UK). The mechanical properties of consistency, cohesiveness, and firmness were assessed for the prepared nanogel using the recommended specifications.[46]

In Vitro Drug Release. For in vitro drug release estimation of an optimized nanogel and non-gelled NLCs formulation dissolution method was performed by employing a dialysis membrane (molecular weight: 12000 Da, Sigma-Aldrich, Merck). The membrane was preactivated using 0.3% w/v sodium sulfide aq. solution at 80 °C to remove sulfur compounds. The treated membrane was washed under running hot water (60 °C) for 2 min, acidified with an aqueous solution of H_2SO_4 (0.2% v/v), rinsed, and immersed in a freshly prepared dissolution medium (VFS) overnight. The formulation samples (10 mL) were placed in preactivated dialysis membranes and immersed in VFS (200 mL) aided by constant stirring at 400 rpm; 37 ± 0.5 °C, magnetic stirrer, Remi Instrument Ltd., Mumbai, India. The aliquots were withdrawn at preset time intervals and replaced with equal VFS to maintain sink conditions.[47,48] The suitably dilute aliquots samples were analyzed at λ_{max}, 296 nm, UV−visible spectrophotometer (UV-1601, Shimadzu).[16] The analysis was performed in triplicate.

Ex Vivo Permeation. Goat vaginal tissue was obtained from a local slaughterhouse, preserved in simulated vaginal fluid (pH 4.5) for transit, and used within 2 h. A thin section of vaginal mucosal tissue was placed between the donor and receptor compartments of Franz diffusion cells. The formulation samples were applied over the mucosal membrane, and the receptor compartments were filled with VSF (9 mL). The assembly was maintained at 37 °C under constant stirring with a magnetic stirrer (Remi Instrument Ltd., Mumbai, India). The aliquots were withdrawn at preset time intervals (0, 1, 2, 4, 8 h) and replaced with VFS to maintain sink conditions.[49,50] The suitably diluted aliquots samples were analyzed at λ_{max}, 300 nm, UV−visible spectrophotometer (UV-1601, Shimadzu).[16] The analysis was performed in triplicate.

Vaginal Irritation. The vaginal irritation studies were carried out using Wistar strain rats (180−200 g)[32] following a duly approved protocol, Institutional Animal Ethics Committee, Jamia Hamdard, India (Protocol no. 1796; Approval Date: March 10, 2021). The animals were divided into three groups: formulation, placebo, and control group. In the formulation group, the rats' vaginal cavities were exposed with the application of an optimized nanogel for 24 h. The placebo group, formulation samples without any drug, was subjected to a similar protocol. No formulation (with or without the drug) was applied in the control group. Following the 24 h formulation exposure period the vaginal cavities application sites were visually scrutinized for erythema and edema using the Draize scales.[31]

Histological Assessment. Post visual examination the animals were sacrificed and the affected skin was excised. The skin samples were preserved in formalin solution (10%v/v) buffered with phosphate buffer saline (pH 7.4). For sectioning, the paraffin blocks of the skin samples were prepared using ethanol and xylene. The sample blocks were microsectioned (5 μm thickness), Microtome, and stained with H&E tissue stain

(hematoxylin and eosin). The prepared sample slides were observed under a microscope (Motic, Japan ix71, Olympus Corporation, Japan) at 10× magnifications.[51]

Anticandidal Activity. *Sample Collection and Laboratory Diagnosis.* Institute approvals: The antifungal activity of the drug was tested on pathogenic strains of *C. albicans*, isolated from a clinical specimen with approval from the Institutional Ethics Committee, Jamia Hamdard, India [Project Title: Design and evaluation of a vaginal drug delivery system (VDDS) for the treatment of candidal vulvovaginitis; Approval Date: April 07, 2022]. High vaginal swabs (HVS samples) were obtained from adult, non-virgin females (18–60 years), with clear symptoms of erythema and itching of the vulva, vagina, or both and cheesy vaginal discharge, after obtaining written informed consent at Unani OPD, Majeedia Hospital, Jamia Hamdard, India. The collected sample was further subjected to microscopy, culture, and isolation of *C. albicans*.[52,53]

Determination of MIC. Three to five well-isolated colonies were mixed with 4–5 mL of RPMI1640 medium supplemented with 2% glucose and were incubated at 35 ± 2 °C for 2–6 h. The turbidity was adjusted to obtain an inoculum concentration of 5×10^5 CFU/mL. The 96-well round-bottom microdilution tray was inoculated with 50 μL of inoculum in each well followed by 50 μL of various dilutions of the drug and formulation. Two wells in each row were used as control, one well contained 100 μL of inoculum (without antifungal) and another had 100 μL of sterile broth. Post incubation (16–20h) the MIC was noted as the lowest concentration of the drug that completely inhibits fungal growth in the microdilution wells as detected by the unaided eye.[54]

C. albicans **Biofilm Model: Establishment of Biofilm.** *C. albicans* biofilm was established on a sterile 96-well microtiter plate using vaginal clinical isolates. A colony of each isolate was inoculated into tubes containing 2 mL of brain heart infusion broth (BHIB) and incubated at 37 °C for 24 h. The broth cultures were diluted using fresh BHIB (ratio-1:2), placed into microtiter plates (200 μL), and incubated at 37 °C for 48 h. The microtiter plates were emptied, rinsed three times with distilled water, and inverted to blot. A 200 μL of 1% crystal violet solution was added to each well and incubated for 15 min. The microplates were rinsed three times using distilled water, and 200 μL of an ethanol/acetone mixture (ratio 8:2) was added to each well. The OD for each well was recorded at 570 nm using an ELISA reader. Sterile BHIB without microorganisms was used as the negative control. The cutoff value was determined by arithmetically averaging the OD of the wells containing sterile BHIB and by adding a standard deviation of +2. The sample with an OD higher and lower than the cutoff value were considered positive, i.e., biofilm-forming, and negative, i.e., non-biofilm forming, respectively.[53]

Antibiofilm Assay. *Determination of MBIC.* The 96-well microtiter plate was prepared with 50 μL of inoculated broth cultures, 50 μL of various dilutions of the drug, and formulation in each well and incubated at 37 °C for 48 h. The plate was emptied, rinsed three times using distilled water, and inverted to blot. 200 μL of 1% crystal violet solution was added to each well and incubated for 15 min. The microplates were rinsed three times using distilled water, and 200 μL of an ethanol/acetone mixture (ratio 8:2) was added. The OD for each well was recorded at 570 nm using an ELISA reader. The samples with an OD higher or lower than the cutoff value were considered biofilm non-inhibiting and biofilm inhibiting,

respectively.[55] An aqueous drug suspension of an optimized formulation was also subjected to a similar protocol.

Determination of MBEC. The 96-well microtiter plate was prepared with 100 μL of inoculated broth cultures in each well and incubated at 37 °C for 48 h. The plate was emptied, and 100 μL of various dilutions of the drug was added to each well and incubated at 37 °C for 24 h. The plate was rinsed three times using distilled water and inverted to blot. 200 μL of 1% crystal violet solution was added to each well and incubated for 15 min. The plate was rinsed again three times using distilled water, and a 200 μL of ethanol/acetone mixture (ratio 8:2) was added. The OD for each well was recorded at 570 nm using an ELISA reader. The samples with an OD higher or lower than the cutoff value were considered biofilm non-eradicating and biofilm eradicating.[33] An aqueous drug suspension of an optimized formulation was also subjected to a similar protocol.

Fluorescence Microscopy. The three different sets of glass slides, one on which the biofilm was allowed to develop in the absence of a drug, those which were incubated in the presence of a drug (to detect inhibition), and those on which biofilm was first allowed to develop before incubation in the presence drugs (to detect eradication), were subjected to fluorescence staining, Calcofluor White Stain (Sigma-Aldrich). The images of biofilm were visualized under a fluorescence microscope (Nikon Eclipse- excitation filter: 340 ± 380 nm, dichroic mirror: 400 nm, and barrier filter: 435 ± 485 nm).[56]

■ AUTHOR INFORMATION

Corresponding Authors

Asgar Ali — *Department of Pharmaceutics, School of Pharmaceutical Education & Research (SPER), Jamia Hamdard, New Delhi 110062, India*; Phone: +91-9899571726; Email: aali@jamiahamdard.ac.in

Zeenat Iqbal — *Department of Pharmaceutics, School of Pharmaceutical Education & Research (SPER), Jamia Hamdard, New Delhi 110062, India*; orcid.org/0000-0003-2788-9420; Phone: +91-9811733016; Email: zeenatiqbal@jamiahamdard.ac.in

Authors

Nazia Hassan — *Department of Pharmaceutics, School of Pharmaceutical Education & Research (SPER), Jamia Hamdard, New Delhi 110062, India*; orcid.org/0000-0001-7264-8103

Uzma Farooq — *Department of Pharmaceutics, School of Pharmaceutical Education & Research (SPER), Jamia Hamdard, New Delhi 110062, India*

Ayan Kumar Das — *Hamdard Institute of Medical Sciences & Research, Jamia Hamdard, New Delhi 110062, India*

Kalicharan Sharma — *Department of Pharmaceutical Chemistry, DPSRU, New Delhi 110017, India*

Mohd. Aamir Mirza — *Department of Pharmaceutics, School of Pharmaceutical Education & Research (SPER), Jamia Hamdard, New Delhi 110062, India*; orcid.org/0000-0002-5780-7601

Suhail Fatima — *Department of Amraz-E-Niswan Wa Qabalat, School of Unani Medical Education & Research (SUMER), Jamia Hamdard, New Delhi 110062, India*

Omana Singh — *Department of Pharmaceutics, School of Pharmaceutical Education & Research (SPER), Jamia Hamdard, New Delhi 110062, India*

Mohammad Javed Ansari − *Department of Pharmaceutics, College of Pharmacy, Prince Sattam Bin Abdulaziz University, Al-Kharj 16278, Saudi Arabia;* ● orcid.org/ 0000-0001-9266-7133

Complete contact information is available at:
https://pubs.acs.org/10.1021/acsomega.2c07718

Notes
The authors declare no competing financial interest.

■ REFERENCES

(1) Donders, G. G.; Sobel, J. D. Candida Vulvovaginitis: A Store with a Buttery and a Show Window. *Mycoses* **2017**, *60* (2), 70−72.

(2) Rodríguez-Cerdeira, C.; Martínez-Herrera, E.; Carnero-Gregorio, M.; López-Barcenas, A.; Fabbrocini, G.; Fida, M.; El-Samahy, M.; González-Cespón, J. L. Pathogenesis and Clinical Relevance of Candida Biofilms in Vulvovaginal Candidiasis. *Front. Microbiol.* **2020**, *11*, No. 544480.

(3) Nobile, C. J.; Johnson, A. D. Candida Albicans Biofilms and Human Disease. *Annu. Rev. Microbiol.* **2015**, *69*, 71−92.

(4) Gulati, M.; Nobile, C. J. Candida Albicans Biofilms: Development, Regulation, and Molecular Mechanisms. *Microbes Infect.* **2016**, *18* (5), 310−321.

(5) Sobel, J. D.; Sobel, R. Current Treatment Options for Vulvovaginal Candidiasis Caused by Azole-Resistant Candida Species. *Expert Opin. Pharmacother.* **2018**, *19* (9), 971−977.

(6) Monk, B. C.; Sagatova, A. A.; Hosseini, P.; Ruma, Y. N.; Wilson, R. K.; Keniya, M. V. Fungal Lanosterol 14α-Demethylase: A Target for next-Generation Antifungal Design. *Biochim. Biophys. Acta BBA-Proteins Proteomics* **2020**, *1868* (3), 140206.

(7) McCall, A. D.; Pathirana, R. U.; Prabhakar, A.; Cullen, P. J.; Edgerton, M. Candida Albicans Biofilm Development Is Governed by Cooperative Attachment and Adhesion Maintenance Proteins. *NPJ. Biofilms Microbiomes* **2019**, *5* (1), 1−12.

(8) Niwano, Y.; Koga, H.; Kodama, H.; Kanai, K.; Miyazaki, T.; Yamaguchi, H. Inhibition of Sterol 14 Alpha-Demethylation of Candida Albicans with NND-502, a Novel Optically Active Imidazole Antimycotic Agent. *Med. Mycol.* **1999**, *37* (5), 351−355.

(9) Taghipour, S.; Kiasat, N.; Shafiei, S.; Halvaeezadeh, M.; Rezaei-Matehkolaei, A.; Mahmoudabadi, A. Z. Luliconazole, a New Antifungal against Candida Species Isolated from Different Sources. *J. Mycol. Medicale* **2018**, *28* (2), 374−378.

(10) Shokoohi, G. R.; Badali, H.; Mirhendi, H.; Ansari, S.; Rezaei-Matehkolaei, A.; Ahmadi, B.; Vaezi, A.; Alshahni, M. M.; Makimura, K. In Vitro Activities of Luliconazole, Lanoconazole, and Efinaconazole Compared with Those of Five Antifungal Drugs against Melanized Fungi and Relatives. *Antimicrob. Agents Chemother.* **2017**, *61* (11), e00635017−e00635-17.

(11) Firdaus, S.; Hassan, N.; Mirza, M. A.; Ara, T.; El-Serehy, H. A.; Al-Misned, F. A.; Iqbal, Z. FbD Directed Fabrication and Investigation of Luliconazole Based SLN Gel for the Amelioration of Candidal Vulvovaginitis: A 2 T (Thermosensitive & Transvaginal). *Approach. Saudi J. Biol. Sci.* **2021**, *28* (1), 317−326.

(12) Salvi, V. R.; Pawar, P. Nanostructured Lipid Carriers (NLC) System: A Novel Drug Targeting Carrier. *J. Drug Delivery Sci. Technol.* **2019**, *51*, 255−267.

(13) Ravi, N. S.; Aslam, R. F.; Veeraraghavan, B. A New Method for Determination of Minimum Biofilm Eradication Concentration for Accurate Antimicrobial Therapy. *Methods Mol. Biol. Clifton NJ.* **2019**, *1946*, 61−67.

(14) Maheronnaghsh, M.; Dehghan, P.; Fatahinia, M.; Rezaei, A. In Vitro Activity of New Azole Luliconazole Compared to Fluconazole against Candida Strains Isolated from Oral Lesions of Cancer Patients. *J. Res. Med. Dent. Sci.* **2019**, *7* (3), 7.

(15) Kaur, M.; Singh, K.; Jain, S. K. Luliconazole Vesicular Based Gel Formulations for Its Enhanced Topical Delivery. *J. Liposome Res.* **2020**, *30*, 388.

(16) Shaikh, M. S.; Kale, M. A.; Mahaparle, P. R.; Rajput, H.; Karkhele, S. M. Development and Validation of UV Spectrophotometric Method for the Estimation of Luliconazole in Bulk, Marketed Formulations. *J. Curr. Pharma Res.* **2020**, *10* (3), 3759−3770.

(17) Jannin, V. THE APPLICATION OF GATTEFOSE PRODUCTS: A 2005−2006 LITERATURE REVIEW. *Bull. Technol.-GATTEFOSSE* **2006**, *99*, 103.

(18) Notario-Pérez, F.; Cazorla-Luna, R.; Martín-Illana, A.; Ruiz-Caro, R.; Peña, J.; Veiga, M.-D. Tenofovir Hot-Melt Granulation Using Gelucire® to Develop Sustained-Release Vaginal Systems for Weekly Protection against Sexual Transmission of HIV. *Pharmaceutics* **2019**, *11* (3), 137.

(19) Khan, S.; Baboota, S.; Ali, J.; Narang, R. S.; Narang, J. K. Chlorogenic Acid Stabilized Nanostructured Lipid Carriers (NLC) of Atorvastatin: Formulation, Design and in Vivo Evaluation. *Drug Dev. Ind. Pharm.* **2016**, *42* (2), 209−220.

(20) Cunha, S.; Costa, C. P.; Moreira, J. N.; Lobo, J. S.; Silva, A. C. Using the Quality by Design (QbD) Approach to Optimize Formulations of Lipid Nanoparticles and Nanoemulsions: A Review. *Nanomedicine Nanotechnol. Biol. Med.* **2020**, *28*, 102206.

(21) Javed, M. N.; Alam, M. S.; Waziri, A.; Pottoo, F. H.; Yadav, A. K.; Hasnain, M. S.; Almalki, F. A. QbD Applications for the Development of Nanopharmaceutical Products. In *Pharmaceutical quality by design*; Elsevier, 2019; pp 229−253.

(22) Khosa, A.; Reddi, S.; Saha, R. N. Nanostructured Lipid Carriers for Site-Specific Drug Delivery. *Biomed. Pharmacother.* **2018**, *103*, 598−613.

(23) Danaei, M.; Dehghankhold, M.; Ataei, S.; Hasanzadeh Davarani, F.; Javanmard, R.; Dokhani, A.; Khorasani, S.; Mozafari, M. Impact of Particle Size and Polydispersity Index on the Clinical Applications of Lipidic Nanocarrier Systems. *Pharmaceutics* **2018**, *10* (2), 57.

(24) Padhi, S.; Mirza, M. A.; Verma, D.; Khuroo, T.; Panda, A. K.; Talegaonkar, S.; Khar, R. K.; Iqbal, Z. Revisiting the Nanoformulation Design Approach for Effective Delivery of Topotecan in Its Stable Form: An Appraisal of Its in Vitro Behavior and Tumor Amelioration Potential. *Drug Delivery* **2016**, *23* (8), 2827−2837.

(25) Lippacher, A.; Müller, R. H.; Mäder, K. Liquid and Semisolid SLN^TM Dispersions for Topical Application: Rheological Characterization. *Eur. J. Pharm. Biopharm.* **2004**, *58* (3), 561−567.

(26) Yu, T.; Malcolm, K.; Woolfson, D.; Jones, D. S.; Andrews, G. P. Vaginal Gel Drug Delivery Systems: Understanding Rheological Characteristics and Performance. *Expert Opin. Drug Delivery* **2011**, *8* (10), 1309−1322.

(27) Palmeira-de-Oliveira, R.; Oliveira, A. S.; Rolo, J.; Tomás, M.; Palmeira-de-Oliveira, A.; Simões, S.; Martinez-de-Oliveira, J. Women's Preferences and Acceptance for Different Drug Delivery Routes and Products. *Adv. Drug Delivery Rev.* **2022**, *182*, 114133.

(28) Machado, R. M.; Palmeira-de-Oliveira, A.; Gaspar, C.; Martinez-de-Oliveira, J.; Palmeira-de-Oliveira, R. Studies and Methodologies on Vaginal Drug Permeation. *Adv. Drug Delivery Rev.* **2015**, *92*, 14−26.

(29) Şenyiğit, Z. A.; Karavana, S. Y.; Eraç, B.; Gürsel, Ö.; Limoncu, M. H.; Baloğlu, E. Evaluation of Chitosan Based Vaginal Bioadhesive Gel Formulations for Antifungal Drugs. *Acta Pharm.* **2014**, *64* (2), 139−156.

(30) Hani, U.; Bhat, R. S.; Sisodiya, R.; Gurumallappa Shivakumar, H. Novel Vaginal Drug Delivery Systems: A Review. *Curr. Drug Ther.* **2010**, *5* (2), 95−104.

(31) Doughty, D. V.; Clawson, C. Z.; Lambert, W.; Subramony, J. A. Understanding Subcutaneous Tissue Pressure for Engineering

Injection Devices for Large-Volume Protein Delivery. *J. Pharm. Sci.* **2016**, *105* (7), 2105−2113.

(32) McCracken, J. M.; Calderon, G. A.; Robinson, A. J.; Sullivan, C. N.; Cosgriff-Hernandez, E.; Hakim, J. C. Animal Models and Alternatives in Vaginal Research: A Comparative Review. *Reprod. Sci.* **2021**, *28* (6), 1759−1773.

(33) Galdiero, E.; de Alteriis, E.; De Natale, A.; D'Alterio, A.; Siciliano, A.; Guida, M.; Lombardi, L.; Falanga, A.; Galdiero, S. Eradication of Candida Albicans Persister Cell Biofilm by the Membranotropic Peptide GH625. *Sci. Rep.* **2020**, *10* (1), 5780.

(34) Kioshima, E. S.; Shinobu-Mesquita, C. S.; Abadio, A. K. R.; Felipe, M. S. S.; Svidzinski, T. I. E.; Maigret, B. Selection of Potential Anti-Adhesion Drugs by in Silico Approaches Targeted to ALS3 from Candida Albicans. *Biotechnol. Lett.* **2019**, *41* (12), 1391−1401.

(35) Kumar, A.; Alam, A.; Grover, S.; Pandey, S.; Tripathi, D.; Kumari, M.; Rani, M.; Singh, A.; Akhter, Y.; Ehtesham, N. Z. Peptidyl-Prolyl Isomerase-B Is Involved in Mycobacterium Tuberculosis Biofilm Formation and a Generic Target for Drug Repurposing-Based Intervention. *Npj Biofilms Microbiomes* **2019**, *5* (1), 1−11.

(36) Ooi, N.; Eady, E. A.; Cove, J. H.; O'Neill, A. J. *Tert*-Butyl Benzoquinone: Mechanism of Biofilm Eradication and Potential for Use as a Topical Antibiofilm Agent. *J. Antimicrob. Chemother.* **2016**, *71* (7), 1841−1844.

(37) Dovnik, A.; Golle, A.; Novak, D.; Arko, D.; Takač, I. Treatment of Vulvovaginal Candidiasis: A Review of the Literature. *Acta Dermatovenerol Alp Pannonica Adriat* **2015**, *24* (1), 5−7.

(38) Tietz, K.; Klein, S. Simulated Genital Tract Fluids and Their Applicability in Drug Release/Dissolution Testing of Vaginal Dosage Forms. *Dissolut Technol.* **2018**, *25* (3), 40−51.

(39) Kovács, A.; Berkó, S.; Csányi, E.; Csóka, I. Development of Nanostructured Lipid Carriers Containing Salicyclic Acid for Dermal Use Based on the Quality by Design Method. *Eur. J. Pharm. Sci.* **2017**, *99*, 246−257.

(40) Subramaniam, B.; Siddik, Z. H.; Nagoor, N. H. Optimization of Nanostructured Lipid Carriers: Understanding the Types, Designs, and Parameters in the Process of Formulations. *J. Nanoparticle Res.* **2020**, *22* (6), 1−29.

(41) Luiz, M. T.; Viegas, J. S. R.; Abriata, J. P.; Viegas, F.; de Carvalho Vicentini, F. T. M.; Bentley, M. V. L. B.; Chorilli, M.; Marchetti, J. M.; Tapia-Blacido, D. R. Design of Experiments (DoE) to Develop and to Optimize Nanoparticles as Drug Delivery Systems. *Eur. J. Pharm. Biopharm.* **2021**, *165*, 127−148.

(42) Verma, D.; Thakur, P. S.; Padhi, S.; Khuroo, T.; Talegaonkar, S.; Iqbal, Z. Design Expert Assisted Nanoformulation Design for Co-Delivery of Topotecan and Thymoquinone: Optimization, in Vitro Characterization and Stability Assessment. *J. Mol. Liq.* **2017**, *242*, 382−394.

(43) Esposito, E. Production, Physico-Chemical Characterization and Biodistribution Studies of Lipid Nanoparticles. *J. Nanomedicine Nanotechnol.* **2015**, *6*, 1 DOI: 10.4172/2157-7439.1000256.

(44) Anzar, N.; Mirza, Mohd. A.; Anwer, K.; Khuroo, T.; Alshetaili, A. S.; Alshahrani, S. M.; Meena, J.; Hasan, N.; Talegaonkar, S.; Panda, A. K.; Iqbal, Z. Preparation, Evaluation and Pharmacokinetic Studies of Spray Dried PLGA Polymeric Submicron Particles of Simvastatin for the Effective Treatment of Breast Cancer. *J. Mol. Liq.* **2018**, *249*, 609−616.

(45) Khuroo, T.; Verma, D.; Khuroo, A.; Ali, A.; Iqbal, Z. Simultaneous Delivery of Paclitaxel and Erlotinib from Dual Drug Loaded PLGA Nanoparticles: Formulation Development, Thorough Optimization and in Vitro Release. *J. Mol. Liq.* **2018**, *257*, 52−68.

(46) Garg, N. K.; Tandel, N.; Bhadada, S. K.; Tyagi, R. K. Nanostructured Lipid Carrier−Mediated Transdermal Delivery of Aceclofenac Hydrogel Present an Effective Therapeutic Approach for Inflammatory Diseases. *Front. Pharmacol.* **2021**, *12*, No. 713616.

(47) Czajkowska-Kośnik, A.; Szekalska, M.; Winnicka, K. Nanostructured Lipid Carriers: A Potential Use for Skin Drug Delivery Systems. *Pharmacol. Rep.* **2019**, *71* (1), 156−166.

(48) Khuroo, T.; Verma, D.; Talegaonkar, S.; Padhi, S.; Panda, A. K.; Iqbal, Z. Topotecan−Tamoxifen Duple PLGA Polymeric Nano-particles: Investigation of in Vitro, in Vivo and Cellular Uptake Potential. *Int. J. Pharm.* **2014**, *473* (1−2), 384−394.

(49) Bondre, R. M.; Kanojiya, P. S.; Wadetwar, R. N.; Kangali, P. S. Sustained Vaginal Delivery of in Situ Gel Containing Voriconazole Nanostructured Lipid Carrier: Formulation, in Vitro and Ex Vivo Evaluation. *J. Dispers. Sci. Technol.* **2022**, 1−13.

(50) Iqbal, Z. Oral Formulation of Paclitaxel and Erlotinib Polymeric Nanoparticles: A Potential Combination to Treat Breast Cancer. *Biomed. J. Sci. Technol. Res.* **2020**, *31* (4), 24338−24340, DOI: 10.26717/BJSTR.2020.31.005129.

(51) Hassan, N.; Singh, M.; Sulaiman, S.; Jain, P.; Sharma, K.; Nandy, S.; Dudeja, M.; Ali, A.; Iqbal, Z. Molecular Docking-Guided Ungual Drug-Delivery Design for Amelioration of Onychomycosis. *ACS Omega* **2019**, *4* (5), 9583−9592.

(52) Hedayati, M. T.; Taheri, Z.; Galinimoghadam, T.; Aghili, S. R.; Cherati, J. Y.; Mosayebi, E. Isolation of Different Species of Candida in Patients with Vulvovaginal Candidiasis from Sari, Iran. *Jundishapur J. Microbiol.* **2015**, *8* (4), 15992 DOI: 10.5812/jjm.8(4)2015.15992.

(53) Marak, M. B.; Dhanashree, B. Antifungal Susceptibility and Biofilm Production of Candida Spp. Isolated from Clinical Samples. *Int. J. Microbiol.* **2018**, *2018*, 1.

(54) Berkow, E. L.; Lockhart, S. R.; Ostrosky-Zeichner, L. Antifungal Susceptibility Testing: Current Approaches. *Clin. Microbiol. Rev.* **2020**, *33* (3), e00069-19.

(55) Zarei Mahmoudabadi, A.; Zarrin, M.; Kiasat, N. Biofilm Formation and Susceptibility to Amphotericin B and Fluconazole in Candida Albicans. *Jundishapur J. Microbiol.* **2014**, *7* (7), e17105 DOI: 10.5812/jjm.17105.

(56) Bogachev, M. I.; Volkov, V. Y.; Markelov, O. A.; Trizna, E. Y.; Baydamshina, D. R.; Melnikov, V.; Murtazina, R. R.; Zelenikhin, P. V.; Sharafutdinov, I. S.; Kayumov, A. R. Fast and Simple Tool for the Quantification of Biofilm-Embedded Cells Sub-Populations from Fluorescent Microscopic Images. *PLoS One* **2018**, *13* (5), No. e0193267.